DOI 10.5162/IMCS2012/P1.0.3

Pt-loaded WO_3 Thick Films for NO_2 Gas sensing

T. Samerjai[1], N. Tamaekong[2], C. Liewhiran[3], A. Wisitsoraat[4], S. Phanichphant[5,*]
[1]Nanoscience and Nanotechnology Program, Graduate School, Chiang Mai University, Chiang Mai, Thailand
[2]Nanoscience Research Laboratory, Faculty of Science, Chiang Mai University, Chiang Mai, Thailand
[3]Department of Physics and Materials Science, Faculty of Science, Chiang Mai, Thailand
[4]Nanoelectronics and MEMS Laboratory, Pathumthani, Thailand
[5]Materials Science Research Center, Faculty of Science, Chiang Mai University, Chiang Mai, Thailand
* Corresponding author: E-mail sphanichphant@yahoo.com

Abstract

Unloaded WO_3 and 0.25–1.0 wt% Pt-loaded WO_3 nanoparticles were synthesized by flame spray pyrolysis (FSP). Tungsten (VI) ethoxide 5% w/v in ethanol 99.8% and platinum (II) acetylacetonate were used as W and Pt precursors respectively. The unloaded WO_3 and 0.25–1.0 wt% Pt-loaded WO_3 nanoparticles were characterized by X-ray diffraction (XRD), scanning electron microscopy (SEM) and High resolution transmission electron microscopy (HR-TEM). The BET surface area (SSA_{BET}) of the nanoparticles was measured by nitrogen adsorption. The thick films on alumina substrate interdigitated with gold electrodes were fabricated by spin-coating technique. The gas sensing characteristics toward NO_2 (1–50 ppm) were performed at the operating temperatures ranging from 150 to 300°C.

Key words: Pt-loaded WO_3 nanoparticles, Flame spray pyrolysis, Nitrogen dioxide (NO_2), Gas sensor, Thick films

Introduction

Tungsten oxide (WO_3) is a wide band-gap n-type semiconductor that has attracted much recent interest as a promising gas sensor because of its excellent sensitivity and selectivity [1]. Platinum (Pt) is a good catalyst that promotes chemical reactions by reducing the activation energy between sensing film and particular gas. Pt can be used to increase response and selectivity as well as to reduce response and recovery times [2]. Moreover, the additives can increase the material porosity, thus increasing the specific surface area suitable for gas adsorption, consequently and the sensor response. The sensor performance can be improved by the incorporation of different additives to the films. In present study, Unloaded WO_3 and 0.25–1.0wt% Pt-loaded WO_3 nanoparticles were synthesized by flame spray pyrolysis (FSP) process and their gas sensing responses towards NO_2 was investigated.

Experimental

1. Flame-made WO_3 nanoparticles

Tungsten ethoxide (Alfa Aesor, 5% w/v in ethanol99.8%) and platinum (II) acetylacetonate ($Pt(acac)_2$, Aldrich, 97% Pt) were used as the W and Pt precursors. FSP was performed as reported in the literature [3].

2. Preparation of sensing films

The sensing films were prepared by mixing the nanoparticles into an organic paste composed of ethyl cellulose (Fluka, 30–60 mPaS) and terpineol (Aldrich, 90%), which acted as a vehicle binder and solvent, respectively. The resulting paste was spin-coated on Al_2O_3 substrates (Semiconductor Wafer, Inc, 96%) interdigitated with Au electrodes. The sensing films were annealed at 400°C for 2 h with the heating rate of 2°C/min for binder removal.

3. Gas sensing measurement

Gas sensing measurements of unloaded WO_3 and Pt-loaded WO_3 sensors were performed in a stainless steel chamber as reported in the literature [2]. NO_2 concentration was varied from 1–50 ppm.

Results and Discussion

1. Particles Properties

The morphology, structure and size of the samples are investigated by SEM. Fig.1 indicates that morphology of the nonoparticles is approximately spherical with the diameter smaller than 50 nm. The EDS spectrum in the inset of Fig. 1 EDS data confirmed the existence of Pt and the Pt content in this region was found to be 1.3 wt%.

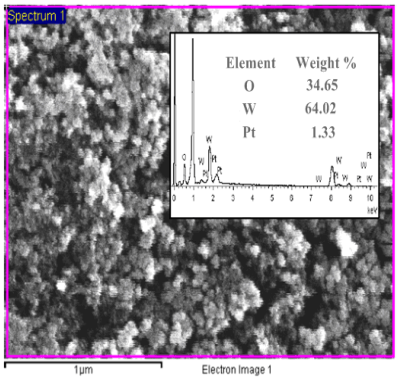

Fig.1. SEM image of the flame-made (5/5) 1.0 wt% Pt-loaded WO_3 nanoparticles.

Fig.2 shows HR-TEM images and SAED patterns of 1.0 wt% Pt-loaded WO_3 nanoparticles. HR-TEM shows that the sample was observed as particles having a clear spherical morphology. The crystallite sizes of spherical 1.0 wt% Pt- loaded WO_3 was found to be ranging from 5–20 nm. Pt nanoparticles are uniformly dispersed on the surface of larger WO_3 particles as marked in circles. The size of Pt nanoparticles was smaller than 1 nm.

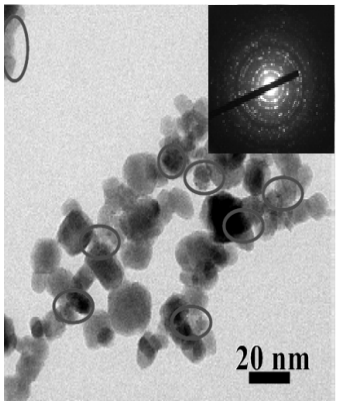

Fig.2. HR-TEM image and SAED pattern of 1.0 wt% Pt-loaded WO_3 nanoparticles.

Fig.3 shows the XRD patterns of as-prepared unloaded and Pt-loaded WO_3 nanoparticles (P0-P1), Au/Al_2O_3 substrate and corresponding WO_3 sensing films after annealing (S0-S1). The P0-P1 samples were highly crystalline and all peaks can be confirmed to be the monoclinic structure of WO_3 (JCPDS file No.83-0950). Pt peaks were not found in these patterns. XRD peaks of sensing films (S0-S1) confirm the presence of monoclinic WO_3 structure of the films. In addition, it is seen that S0-S1 had different XRD peak intensities compared corresponding nanoparticles (P0-P1), indicating changes in texturization of the crystal plane orientation after sensing films preparation.

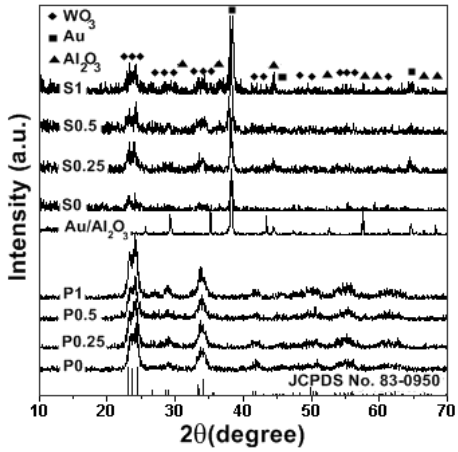

Fig.3. XRD patterns of as-prepared undoped WO_3 (P0), 0.25–1.0 wt% Pt-loaded WO_3 (P0.25-P1), Au/Al_2O_3 substrate, and samples P0, P0.25, P0.5, and P1 were spin-coated on Au/Al_2O_3 substrat, S0.5, and S1) ((◆) WO_3; (▲) Al_2O_3; (■) Au).

The specific surface areas (SSA_{BET}) from BET method of unloaded WO_3 and Pt-loaded WO_3 nanoparticles containing 0.25, 0.5 and 1.0 wt% Pt were found to be 84.1, 96.6, 94.9 and 96.2 m^2/g, respectively. The average BET equivalent particle diameters (d_{BET}) were calculated using the densities of WO_3 [4] and Pt [5] taking into account for their weight contents of different loadings. It was found that the calculated particle sizes of all samples were in the same range of 9–11 nm.

2. Gas Sensing Properties

The interaction of the resistive sensors with a target gas produces a change in the electrical conductance of the sensors recorded by a variation in the electrical resistance. The gas-sensing response, S, is defined as the ratio of R_g/R_a where R_g is the resistance in test gas, and R_a is the resistance in dry air. The response time (T_{res}) is defined as the time required until 90% of the response signal is reached. Fig. 4 illustrates the change in resistance of sensors, S0-S1, under exposure to NO_2 gas with different concentrations ranging from 1 to 50 ppm at 150°C. The decrease of

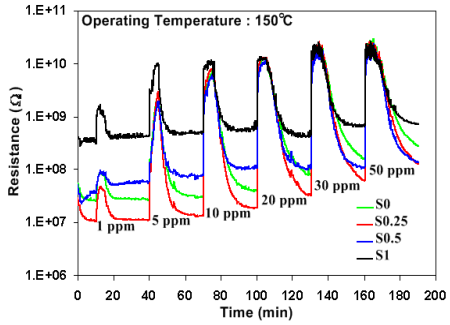

Fig.4. The change in resistance of sensors, S0-S1, under exposure to NO_2 pulses with different concentrations ranging from 1 to 50 ppm at 150°C.

resistance was clearly specified at all gas concentrations indicating that the WO_3 sensor had typical n-type semiconductor behavior. However, the decrease in resistance was small and the recovery speed was slow for unloaded material. The response of unloaded WO_3 (S0) thick film of 327 was observed towards 20 ppm of NO_2 at 150°C as shown in Fig. 5. On Loading with Pt catalysts the gas response was enhanced. It can be seen that sensor S0.25 (0.25%Pt) showed better response than sensor S0.5 (0.5%Pt) and S1 (1.0%Pt). In addition, the response of sensor S0.25 (0.25%Pt) was found to be 954 towards NO_2 concentration of 20 ppm. The response time of NO_2 was less than 2 min. Thus, small Pt loading could greatly improve response towards NO_2. The peculiar feature of the response of the Pt-loaded WO_3 sensor towards NO_2 gas could be caused by two competitive effects: (1) direct adsorption of charge carriers from film conduction band generates the initial increase of the sensor resistance upon exposure of NO_2 gas with high oxidizing power. (2) desorption of oxygen species (O^-, O_2^-, O_2^{2-}), precedently ionosorbed onto film surface, with consequent release of charge carriers to the film conduction band generates the decrease of the resistance of the sensor upon NO_2 gas exposure [6].

The effect of operating temperature on NO_2 response at 10 ppm for WO_3 sensors with different Pt doping concentrations is shown in Fig. 6. It can be seen that the all sensors showed the high response at low operating temperature of 150°C and the response considerably decreases as operating temperature increases. Therefore, optimal operating temperature of 150°C was chosen for NO_2. This is in agreement with other reports that the temperature for the maximum response to NO_x corresponds to about 150°C for Pt/WO_3 [6]. From the experimental results, it was found

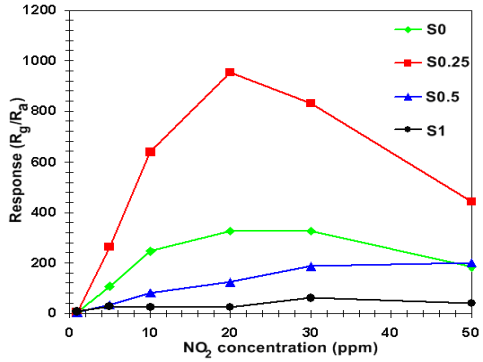

Fig.5. The relative of response with concentration of NO_2 (ppm) between unloaded WO_3 and 0.25–1.0 wt% Pt-loaded WO_3 sensors at 150°C.

that sensor S0.25 showed the highest response of 637 towards 10 ppm of NO_2 at 150°C. Comparing with the same material, Penza et al. [6] reported that the highest sensing behavior towards 10 ppm NO_2 was about 3.45. Also Srivastava et al. [7] reported the Pt-doped WO_3 film prepared by screen-printing, and the sensing test at 450°C with NO_2 at concentration ranging from 40–400 ppm. A sensor showed the highest sensor signal at 400 ppm (S = ~4).

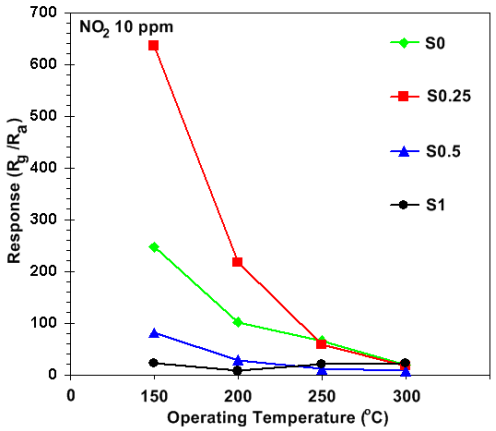

Fig.6. Response versus operating temperature curve for unloaded WO_3 and 0.25–1.0 wt% Pt-loaded WO_3 sensors.

Conclusions

Unloaded WO_3 and Pt-loaded WO_3 (0.25–1.0 wt%) nanoparticles were successfully synthesized by FSP. The XRD patterns revealed that Pt-loaded WO_3 nanoparticles and their corresponding sensing films were crystalline with a monoclinic phase of WO_3. The HR-TEM images showed the nanoparticles having clear spherical morphology. The crystallite sizes of spherical unloaded WO_3 and 1.0 wt% Pt-loaded WO_3 were found to be ranging from 5–20 nm. For Pt-loaded WO_3

powder, spherical Pt nanoparticles were found to disperse over the surface of WO_3 matrix and the presence of Pt element was confirmed by EDS analysis. The sensor performance of spin coated WO_3 thick film-based NO_2 sensor was enhanced by Pt loading. It was found that the 0.25 wt.% Pt-loaded WO_3 sensing film showed an optimum NO_2 response of ~950 towards 20 ppm of NO_2 at 150°C.

Acknowledgements

T.S. and N.T. would like to acknowledge the financial support from the Office of the Higher Education Commission, under the program Strategic Scholarships for Frontier Research Network, Thailand for the Ph.D. scholarship. The National Research University Project under Thailand's Office of the Higher Education Commission, the Graduate School and Department of Chemistry, Faculty of Science, Chiang Mai University, Thailand are gratefully acknowledged.

References

[1] SC. Moulzolf, S.A. Ding, RJ. Lad, Sens. Actuators B, 375–382 (2001); doi: 10.1016/s0925-4005 (01) 00757–2.

[2] N. Tamaekong, C. Liewhiran, A. Wisitsoraat , S. Phanichphant , Sens. Actuatuators B, 155–161 (2011); doi: 10.1016/j.snb.2010.11.058.

[3] T. Samerjai, N. Tamaekong, C. Liewhiran, A. Wisitsoraat , A. Tuantranont, S. Phanichphant , Sens. Actuatuators B, 290–297 (2011); doi: 10.1016/j.snb.2011.03.065.

[4] A. Aird, M.C. Domeneghetti , F. Mazzi, V. Tazzoli, E.K.H. Salje, J. Phys. Condens. Matter, 569–574 (1998); doi: 10.1088/0953-8984/10/33/002.

[5] S.S. Zumdahl, S.L. Zumdahl, D.J. Decoste, World of Chemistry. Houghton Mifflin Company, Boston, 141 (2002); doi: 10.1009/0618249087.

[6] M. Penza. C. Martucci, G. Cassano, Sens. Actuators B, 9–18 (1998).

[7] V. Srivastava, K. Jain, Sens. Actuators B, 46–52 (2008).